Wetting of Lubricants on Cemented Tungsten Carbide Surfaces with Surface Structures Produced with Ultrashort Laser Pulses

Kathrin Placzek*[1], Daniel Holder[1], Oliver Schwarz[2], Rudolf Weber[1], and Thomas Graf[1]

[1]*Institut für Strahlwerkzeuge (IFSW), University of Stuttgart, Germany*
[2] *Institut für Produktionstechnik und Automatisierung (IPA), Fraunhofer, Germany*
Corresponding author's e-mail: kathrin.placzek@ifsw.uni-stuttgart.de

In the presented work, surface structures were generated on cemented tungsten carbide surfaces using ultrashort laser pulses. The type of surface structures was varied by varying the spatial overlap of the laser pulses by using different feed rates while keeping the maximum average power of 10.76 W and the constant repetition rate of 500 kHz. Larger surface structures with increasing roughness could be created by increasing the pulse overlap. The contact angle was measured 30 days after structuring to consider aging. Decreasing contact angles were measured on surfaces of increasing roughness for deionized water. A contact angle of 0° was measured for deionized water on the roughest structure. The same rough surface also resulted in a low contact angle of 8° for a lubricant based on a fatty alcohol and for a water-based lubricant. Therefore, superhydrophilic behavior as well as high wetting of the two lubricants could be demonstrated.

DOI: 10.2961/jlmn.2023.01.2005
Keywords: surface structures, ultrashort laser pulses, water-based lubricants, wetting, micromachining, cemented tungsten carbide

1. Introduction

The wetting of the tool surface with lubricants during the mechanical milling process is essential for obtaining workpieces of high quality. Lubricants are designed to improve the tribology of the tool-workpiece-system. They cool the tool and create reaction layers between the chip and the cutting edge, which reduce friction and wear [1]. Good wetting of the lubricant or a high wettability of the tool surface is mandatory for achieving these lubrification properties. Today, the conventional lubricants based on a fatty alcohol can be replaced by water-based lubricants.

The wettability of the milling tool can be improved by applying surface structures. Ultrashort pulsed laser radiation is a useful tool to produce surface structures in the micro- and nanometer range, which increase the wettability of a surface [2], [3].

The contact angle θ_c is often used to characterize the wettability of a surface. In the case of water, a surface providing a contact angle of $\theta_c > 150°$ is called superhydrophobic. The respective wetting states are called hydrophobic if $\theta_c > 90°$, hydrophilic if $\theta_c < 90°$ and superhydrophilic if $\theta_c \leq 10°$. The contact angle of water on metallic surfaces is typically in the hydrophilic range of $49° < \theta_c < 83°$ [4], [5], [6].

The contact angle depends on the properties of the liquid, such as the surface tension, as well as on the surface topography of the wetted area. Structuring surfaces with ultrashort laser pulses can lead to a time-dependent change in wetting properties [4], [6]. Directly after surface structuring the surfaces are superhydrophilic. A few days up to a few weeks after structuring, the contact angle increases and the wetting state changes to hydrophobic or even superhydrophobic [4], [7]. The cause of this has not yet been fully clarified. *Kietzig et al.* concluded that in addition to the liquid properties and the surface topography the surface chemistry influences the wettability of a surface. The surface chemistry depends on the storing atmosphere [6], the cleaning agent [5], and the time after structuring [7]. In the case of laser micromachining, the surface topography is influenced by the laser-induced surface structure [4]. Different types of surface structures are formed depending on the scanning speed during structuring [8], [9], such as *laser-induced periodic surface structures* (LIPSS) [2] and so called cauliflower-like surface structures with a flaky appearance [10].

In this work different types of surface structures in the micrometer range on cemented tungsten carbide are presented, which show hydrophilic up to superhydrophilic wetting states, as well as low contact angles of different lubricants.

2. Experimental setup and measuring methods

An ultrafast laser system *Duetto* from *Time-Bandwidth* was used for the experiments, which emits laser pulses with a wavelength of 1064 nm and a pulse duration of 10 ps. The laser beam had a Gaussian intensity distribution, was circularly polarized, and had a beam quality factor of $M^2 < 1.3$. The beam was positioned and scanned over the sample surface with a Galvanometer-Scanner and focused by a F-Theta lens with a focal length of 80 mm. The resulting focus diameter was $d_0 = 30 \pm 2$ µm. For all experiments the focus of the beam was set on the surface of the sample.

The tungsten carbide samples (DK460UF from *Gühring*) are made of 90% tungsten carbide and 10% cobalt. with an average size of the tungsten carbide grains of 0.65 µm. The cylindrical sample has a diameter of 20 mm and a thickness of 7 mm. The sample surface was mechanically polished before structuring. Squared areas with a size of 6.5 mm x 6.5 mm and different surface structures were produced on the samples using one scan. The spatial overlap of the pulses, O_p, vas varied by using different feed rates v_s.

Table 1 Feed v_s, pulse overlap O_p and effective energy input E_{eff}

v_s [mm/s]	O_p [%]	E_{eff} [J/cm²]
3747	75	122
1500	90	305
300	98	1523
60	99.6	7617

The hatch distance was kept constant at a_h = 6 µm, as well as the average power of 10.75 W and the repetition rate f_{rep} = 500 kHz. The special overlap O_p of the pulses and special overlap perpendicular to the feed direction O_y are given by

$$O_p = 1 - \frac{v_s}{f_{rep} \cdot d_f} \quad (1)$$

and

$$O_y = 1 - \frac{a_h}{d_f} \quad (2)$$

Together with the peak fluence per burst Φ_0 the effective energy input is given by

$$E_{eff} = \Phi_0 \cdot \frac{1}{(1-O_p)\cdot(1-O_y)} \quad (3)$$

The scan velocity used as well as the resulting pulse overlap and the effective energy input for structuring are listed in Table 1.

The experiments were performed using single pulses and using bursts with five pulses. The bursts have an intra burst time lag of 12 ns.

The resulting surface structures were investigated using a scanning electron microscope (SEM). The structures were characterized by measuring the roughness S_a with a laser scanning microscope (LSM). Furthermore, the structures were analyzed by an energy dispersive X-ray spectroscopy device (EDX).

The wettability of the generated surface structures was determined with a contact angle measuring device. With the dosing unit a droplet with a volume of 1 µL and a dosing rate of 2 µL/s was placed on each surface structure and the contact angle determined after t_x seconds. The sample was cleaned with acetone in an ultrasonic bath after each contact angle measurement. The contact angle was measured regularly 30 days after structuring to consider aging. The contact angle of commercial lubricant based on a fatty alcohol (*ECO CU*T by *Fuchs*) and a water-based lubricant (under development by *HPM*) was measured as described above. For reference, the contact angle of deionized water was measured.

3. Results and discussion

3.1 Characterization of type and roughness of the generated surface structures

The resulting surface structures created with various pulse overlaps O_p are shown in Figure 1. The left column (a)-d)) shows the generated structures using single pulses and the right column (e)-h)) shows the generated structures using burst mode pulses. The corresponding roughness S_a and the measured carbon content of the generated structure as a function of the effective energy input E_{eff} for the generation of the structures is shown in Figure 2.

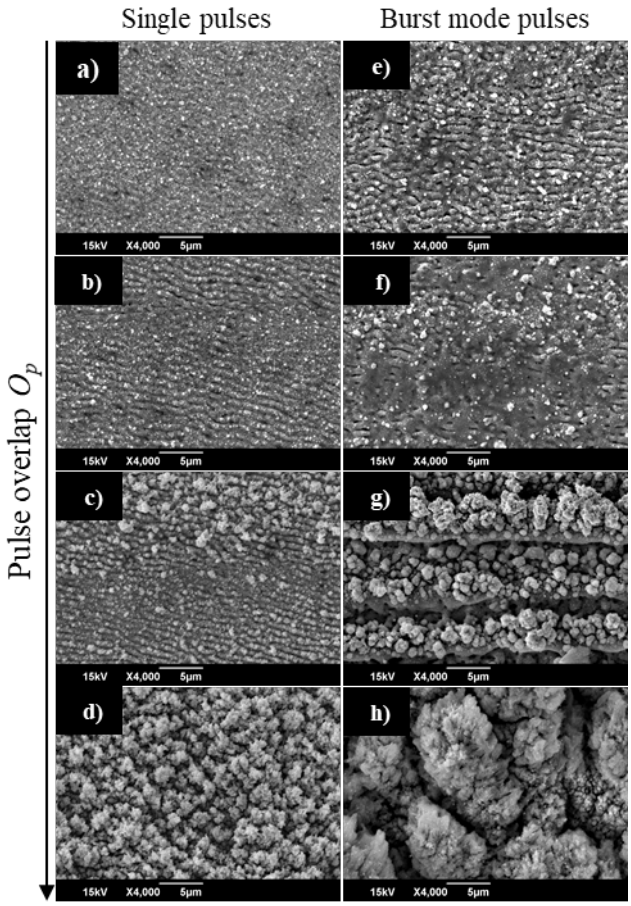

Fig. 1 SEM images of structured surfaces on cemented tungsten carbide using single pulses (left column) and using burst mode pulses (right column) with E_p = 21.5 µJ, Φ_0 = 6.1 J/cm², f_{rep} = 500 kHz and varying pulse overlaps: a) + e) O_p = 75 % ; b) + f) O_p = 90 %; c) + g) O_p = 98 %; d) – h) O_p = 99.6 %.

When using burst mode pulses instead of single pulses with the same total pulse energy significant differences in the type of structure created can be seen. With a pulse overlap of O_p = 75 % single pulses generate no specific structure. In comparison, LIPSS were generated by using five pulses per burst and identical pulse overlap. However, the measured roughness of these structures is at the same value of S_a = 0.46 ± 0.05 µm. With increasing pulse overlap and increasing effective energy input, the measured surface roughness increases, which corresponds well with the results from [7]. The structures generated with a pulse overlap of O_p = 99.6 % show significantly rougher surface structures: the SEM images of the single-pulse surface shows smaller cauliflower-like structure (Figure 1 d)) whereas the surface generated with bursts shows larger cauliflower-like structures (Figure 1 h)). The structure shown in h) is about three times rougher than the single-pulse surface. Figure 1 c) shows that with a pulse overlap O_p = 98 % and using single pulses a transitional structure is formed: LIPSS as well as cauliflower-like structures can be seen. For bursts the appearance of the effect is not that severe, but still can be seen at a pulse overlap of O_p = 90 % (Figure f)). For single pulses the value of the roughness increases and deviates from the initially linear course at O_p = 98 %. The increasing roughness with increasing pulse overlap presumably results from

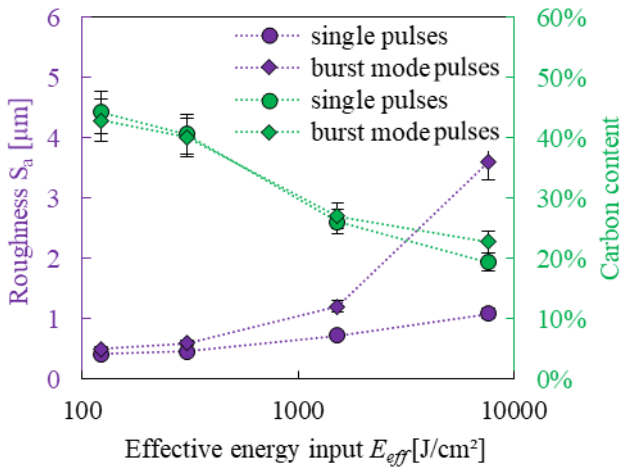

Fig. 2 Roughness S_a of the surface structures and by EDX measured carbon content as a function of the effective energy input E_{eff}. The dotted lines were added to guide the eye.

heat accumulation of subsequent pulses. The effect of heat accumulation can be quantitatively described by a simple model as demonstrated in [11] for metals. With each pulse, residual heat remains in the component. Ultra-short pulse laser ablation with multiple pulses leads to temperature rises, to heat accumulation, melt formation, and therefore to rougher surfaces. The temperature rise depends on the applied energy per spot, which can be determined by the scan velocity, the pulse overlap and the pulse energy [11]. Following this interpretation, the transition structures can be explained by exceeding a critical temperature during laser ablation. Bursts enhance this effect, as the transition structure occurs at lower pulse overlaps than with single pulse ablation.

Figure 2 shows that with increasing roughness of the surface the measured carbon content of the structure decreases. The carbon content is similar for the same effective energy input, regardless of whether bursts were used or not. The roughness of the different structures increases with increasing effective energy input. The increase of the roughness of the structure is greater when using burst mode pulses instead of single pulses.

Figure 3 shows the content of the elements determined with EDX on an unstructured surface (reference) and on surfaces

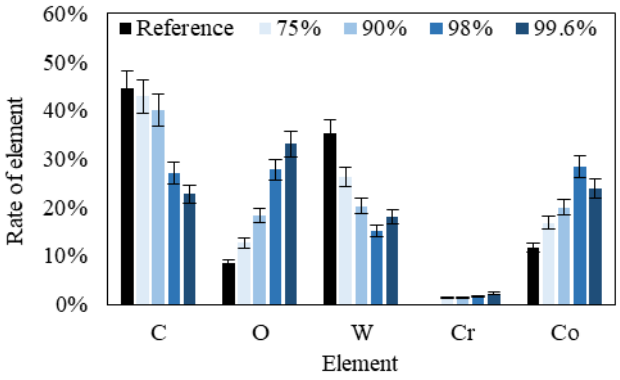

Fig. 3 Content of the elements carbon, oxygen, tungsten, chrome, and cobalt determined on the surface structures generated with various pulse overlaps O_p and burst mode pulses (blue shades) and an unstructured surface (black).

using burst mode pulses and various pulse overlaps O_p. The oxygen and the cobalt content increase with increasing pulse overlap. The tungsten content of the surface decreases with increasing pulse overlaps and with increasing effective pulse energy. Another aspect is the appearance of chrome on the structured surfaces whereas on the unstructured surface no chrome content was detected.

In [11], a correlation between the roughness of the ablated surface structures and their oxygen content was found, too. Energy dispersive X-ray spectroscopy analysis of ablated surfaces on stainless steel showed that rough and bumpy structures had a significantly higher oxygen content. The oxidation of metals is a temperature sensitive effect [11] and thus the larger amount of oxides on the cauliflower-like structures may have been caused by higher temperatures during machining.

3.2 Aging of the surface structures

The contact angles, which were measured for deionized water (DI) on the different surface structures as a function of the day after structuring are shown in Figure 4. The measured contact angle of DI on an unstructured sample is $\theta_c = 52°$ and is shown with a green line in Figure 4 for reference. Low contact angles of up to $\theta_c < 12°$ could be measured for all surfaces on the day the sample was structured, except for the structure created by a pulse overlap $O_p = 75$ % and using single pulses. A contact angle of $\theta_c = 51°$ was measured on this structure on the day of structuring. When using burst mode pulses and a pulse overlap $O_p = 75$ % the contact angle increases on the second day after structuring and remains constant at a contact angle of $\theta_{c;5;75\%} = 57° \pm 5°$. On the structures created with single pulses and a pulse overlap of $O_p = 75$ % and $O_p = 98$ % an increasing contact angle was measured, too. Yet, the course does not remains constant but fluctuates between $\theta_{c;1;75\%;min} = 63°$ and $\theta_{c;1;75\%;max} = 95°$ and $\theta_{c;1;98\%;min} = 37°$ and $\theta_{c;1;98\%;max} = 74°$

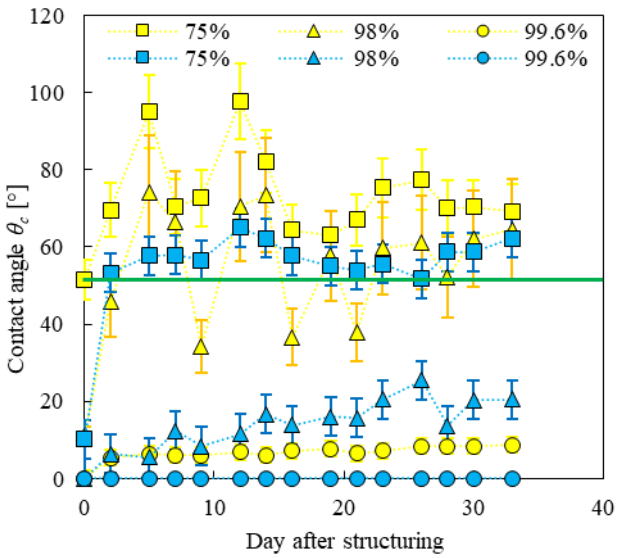

Fig. 4 Contact angle θ_c of deionized water (DI) on surface structures generated by various pulse overlaps and using single pulses (yellow) and burst mode pulses (blue) as a function of the day after structuring. The error bars of the $O_p = 98\%$-curve are orange instead of yellow to provide better visibility.

for a pulse overlap $O_p = 75$ % and $O_p = 98$ %, respectively.

As mentioned previously, for O_p = 98 % using single pulses, a transition structure was formed (see Figure 1 c)). The formation of a transition structure could be an explanation for the fluctuation of some contact angle courses. However, the fluctuating course can also be seen for O_p = 75 %, where no transition structure has formed. The cause of this behavior is not yet clear. The contact angle for both structures remained constant at θ_c = 67° ± 4° 22 days after structuring.

Structuring with higher pulse overlaps, which corresponds to rougher structures, led to lower contact angle of DI on these structures. For the structures generated by a pulse overlap O_p = 99.6 % using single pulses a constant contact angle of θ_c = 8° was measured. With the same parameter selection only using burst mode pulses, which corresponds to the roughest structure, a constant contact angle of θ_c = 0° as measured. Overall, for structures created by a pulse overlap of O_p = 99.6 % regardless of the number of bursts and for the structure generated by O_p = 98 % and using burst mode pulses super hydrophilic behavior could be demonstrated for DI. Figure 5 shows the contact angle θ_c for the surface structures 33 days after structuring (aged state) as a function of the roughness S_a. Structures of low roughness (S_a <1 µm), which show LIPSS or no specific type of structures, led to high contact angles in the range of 58° to 70°. For rougher structures S_a > 1 µm with a cauliflower-like structure and large wetting area, the contact angle decreases abruptly. As a result, durable hydrophilic and superhydrophilic wetting behavior could be demonstrated.

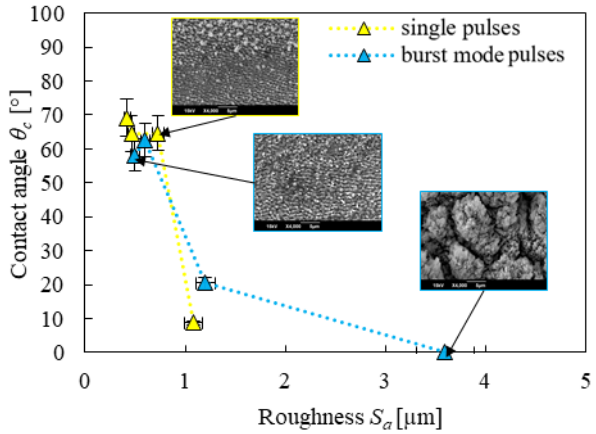

Fig. 5 Contact angle θ_c of deionized water (DI) on different surface structures generated with single pulses (yellow) and burst mode pulses (blue) as a function of the roughness S_a 31 days after structuring

3.3 Contact angle of lubricants

As lubricants, unlike DI, have been developed to provide a high level of wetting regardless of the surface structure of the tool, the expected contact angle of a lubricant on an unstructured surface is relatively low. In order to evaluate the wetting behavior of the two different lubricants on the surface structures, the contact angle was measured frequently up to 15 seconds after the droplet was dropped on the sample surface. Figure 6 and Figure 7 show the change of the contact angle as a function of the time after droplet placement for a lubricant based on a fatty alcohol (FABL) and for a water-based lubricant (WBL). The course of the contact angle for a droplet placed on an unstructured surface is shown as a reference as well as the course of the contact angle measured on the generated structures.

Both figures show, that the contact angle of the lubricants on structured surfaces is significantly lower than the contact angle measured on the unstructured samples (reference). Yet the measured contact angles show different courses over time:

For the FABL, the courses of the contact angle of $\theta_{c;1;75\%}$, $\theta_{c;1;99.6\%}$ and $\theta_{c;5;75\%}$ over time are in a similar range up to t_d = 8 s. The contact angle decreases from θ_c = 11.5±0.4° at t_d = 1 s to θ_c = 5±0.5° at td = 8 s. The course of the contact angle for the roughest structure generated by O_p = 99.6 % and using burst mode $\theta_{c;5;99.6\%}$ is lower. It decreases from θ_c = 9.1° at t_d = 1 s to θ_c = 0° at t_d = 8 s. The reference contact angle measured at t_d = 1 s decreases from θ_c = 18.8° to θ_c = 9.9° at t_d = 11 s. As a result, the contact angle of a lubricant based on a fatty alcohol could be reduced by at least 50 % through micro structuring, which corresponds to an absolute reduction of the contact angle of $\Delta\theta_c$ = 9.5±0.4°.

For the WBL, the courses of the contact angle of the structured surfaces over time are in a similar range up to t_d = 3 s. The contact angle decreases from θ_c = 9.5±1° at t_d = 1 s to θ_c = 5.5±0.6° at td = 3 s. At td = 5 s a contact angle of θ_c = 0° was measured for the surface structures generated by N_b = 5 bursts, whereas the contact angle on the surface structures generated using single pulses was θ_c = 3.7±0.5°. At $t_d \geq$ 8 s a contact angle of θ_c = 0° was determined for all structured surfaces. The reference contact angle measured at t_d = 1 s decreases from θ_c = 19.4° to θ_c = 10.5° at t_d = 11 s. As a result, the contact angle of a water-based lubricant could be reduced by at least 50 % through surface structuring, too.

Comparing the wetting behavior of the two lubricants on the structured surfaces over time after droplet placement commonalities as well as differences can be identified. The investigated fluids have a similar course of the reference contact angle over time. Thus, the water-based lubricant is

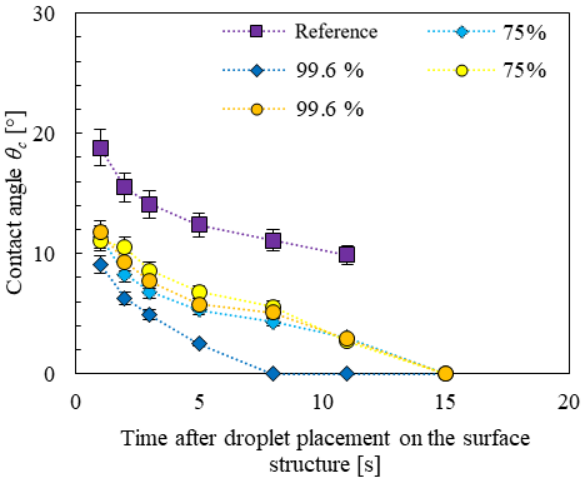

Fig. 6 Contact angle θ_c of a lubricant based on a fatty alcohol as a function of the time after droplet placement on different surface structures: an unstructured surface (purple), structures generated with burst mode pulses (blue) and single pulses (yellow) with a pulse overlap O_p = 75 % and O_p = 99.6 %, respectively.

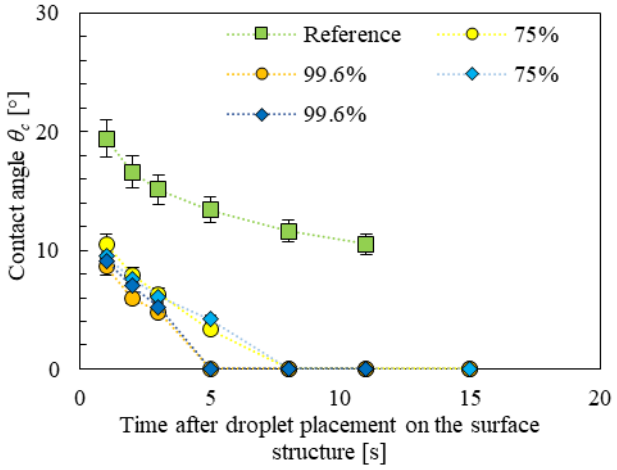

Fig. 7 Contact angle θ_c of a waterbased lubricant as a function of the time after droplet placement on different surface structures: an unstructured surface (green), structures generated with burst mode pulses (blue) and single pulses (yellow) with a pulse overlap O_p = 75 % and O_p = 99.6 %, respectively.

in no way inferior to the conventional lubricant in terms of wetting. By generating the presented surface structures, the contact angle can be reduced significantly. In the first second after droplet placement the contact angle of the structured surfaces is about 10°. Differences show up in the change of the contact angle over time. While using the WBL led to a contact angle θ_c = 0° at t_d = 8 s, using the FABL only on the surface structure created by using a pulse overlap O_p = 99.6 % and burst mode pulses resulted in a contact angle of θ_c = 0° at t_d = 8 s. Accordingly, with regard to the contact angle change over time a faster wetting of the structured surfaces can be observed when using WBL.

As a result, by creating surface structures an improvement of the wetting behavior of lubricants on cemented tungsten carbide surfaces could be achieved. While on unstructured surfaces in t_d < 10 s a minimum contact angle of θ_c = 11° was achieved, in the case of the WBL a contact angle of θ_c = 0° was measured at the same time.

The contact angle or Young's contact angle is used to quantify the wetting states. The Young's model provides a relationship between the prevailing surface tensions and the contact angle formed by a drop of liquid placed on a solid sample and thus allows predictions on the quantification of the different types of wetting. The force mechanism of the surface tension varies depending on the fluid. In oils, Van der Waals forces operate and generate intermolecular energies. These have comparatively low surface tensions of about 20 mN/m. Water, on the other hand, has a relatively high surface tension of 72 mN/m, which is caused by the covalent bonds of the H_2 molecules and is also known as hydrogen bonding [12].

4. Conclusion

In summary, high wetting of deionized water, a lubricant based on a fatty alcohol and a water-based lubricant on cemented tungsten carbide was demonstrated by generating different types of structures using ultra short laser pulses and burst mode pulses as well as single pulses.

The pulse overlap has been varied and single pulses as well as burst mode pulses have been used in order to achieve different types of structures and varying roughness of the structures. With five pulses per burst and by increasing the pulse overlap rougher structures could be produced. While lower pulse overlaps formed LIPSS, higher pulse overlaps led to flaky structures. In addition, transition structures have been identified, which show cauliflower-like surfaces as well as LIPSS. Using a pulse overlap O_p = 99.6 % and five pulses per burst the roughest structure with S_a = 3.4 µm was created. The results of the EDX measurements show that the oxygen content increases and the carbon content decreases th rougher the surface structure.

Finally, the wetting behavior of the generated surface structures was evaluated for deionized water and different lubricants. In the case of deionized water decreasing contact angles could be determined for rougher structures. For these structures it was not necessary to consider aging, as the contact angle remained constant. In contrast, for the smoother structures a stagnation of the contact angle has been determined after above 30 days. For deionized water a constant contact angle of θ_c = 0° was measured on the roughest structure, which corresponds to a superhydrophilic wettability. In the case of the lubricants, it was also possible to generate lower contact angles by structuring. Hereby, the contact angle could be reduced by at least 50 % compared to the contact angle of lubricants on an unstructured sample. Compared to the conventional lubricant, the water-based lubricant showed a faster wetting of the surface structures. The contact angle dropped from θ_c = 10° to θ_c = 0° in t_d = 5 s and t_d = 8 s after droplet placement on the structures created by a pulse overlap of O_p = 99.6 % and O_p = 75 %, respectively.

Acknowledgments

This work was funded by the Federal Ministry for Economic Affairs and Climate Action (BMWK) in the frame of the project “BionicTools” (03EN4007G). Furthermore, the authors thank Liane Hoster for the support with the SEM images.

References

[1] S. Debnath, M. Reddy, and Q. Yi: J. Clean. Prod., 83, (2014) 33.
[2] J. Bonse, S. Höhm, S. Kirner, A. Rosenfeld, and J. Kruger: IEEE J Sel Top Quantum Electron, 23, (2017) 1.
[3] A. Cunha, A. Serro, V. Oliveira, A. Almeida, R. Vilar, and M.-C. Durrieu: Appl. Surf. Sci., 265, (2013) 688.
[4] A.-M. Kietzig, S. Hatzikiriakos, and P. Englezos: Langmuir. 825, (2009) 4821.
[5] G. Schnell, C. Polley, S. Bartling, and H. Seitz: ACS Appl. Nano Mater., 10, (2020) 1241.
[6] D. Huerta-Murillo, A. García-Girón, J. Romano, J. Cardoso, F. Cordovilla, M. Walker, S. Dimov, and J. Ocaña: Appl. Surf. Sci., 463, (2019) 838.
[7] D. Holder, F. Hetzel, R. Weber, and T. Graf: Procedia CIRP, 111, (2022) 715.
[8] F. Bauer, A. Michalowski, and S. Nolte: J. Laser Micro Nanoeng., 10, (2015) 325.
[9] D. Holder, M. Buser, A. Leis, R. Weber, and T. Graf: IOP Conf Ser.: Mater Sci Eng, 1135, (2021) 12005.

[10] S. Zouaghi, T. Six, S. Bellayer, S. Moradi, S. Hatzikiriakos, T. Dargent, V. Thomy, Y. Coffinier, C. André, G. Delaplace, and M. Jimenez: CS Appl. Mater. Interfaces. 319, (2017) 26565.
[11] F. Bauer, A. Michalowski, T. Kiedrowski, and S. Nolte: Opt. Express, 23, (2015) 1035.
[12] A. Marchand, J. Weijs, J. Snoeijer, and B. Andreotti: Am J Phys, 79, (2011) 999.

(Received: July 14, 2022, Accepted: February 12, 2023)